16. Yang Y., Guo X., Wang N. Power generation from pulverized coal in China. *Energy*. 2010. Vol. 35. Iss. 11. P. 4336–4348. https://doi.org/10.1016/j.energy.2009.05.006.
17. Бабенко И. А., Шульгин В. Л. Технологии суперсверхкритических параметров пара в современной энергетике. *Тр. третьей науч.-техн. конф. молодых ученых Урал. энерг. ин-та.* Екатеринбург: Урал. физ. ун-т. 2018. С. 69–71.
18. Лыхвар Н. В., Говорущенко Ю. Н., Яковлев В. А. Моделирование теплоэнергетических установок с использованием интерактивной схемной графики. Пробл. машиностроения. 2003. Т. 6. № 1. С. 30–41.
19. Бабенко О. А. Гибкие математические модели для совершенствования режимов отпуска теплоты теплофикационными блоками ТЭЦ. *Энергосбережение. Энергетика. Энергоаудит*. 2011. № 10. С. 36–40.
20. Rusanov A. V., Shubenko A. L., Senetskyi O. V., Babenko O. A., Rusanov R. A. Heating modes and design optimization of cogeneration steam turbines of powerful units of combined heat and power plant. *Energetika*. 2019. No. 65 (1). P. 39–50. https://doi.org/10.6001/energetika.v65i1.3974.
21. Горпинко Ю. И., Сенецкий А. В., Сарапин В. П., Шубенко А. Л., Маляренко В. А. Двухконтурный термодинамический цикл с однонаправленным теплообменом между холодильным и энергетическим циклами. *Пробл. регион. энергетики.* 2019. № 3 (44). С. 51–64.

DOI: https://doi.org/10.15407/pmach2021.04.049

UDC 539. 3

VIBRATIONS OF A CYLINDRICAL SANDWICH SHELL WITH A HONEYCOMB CORE MADE USING FDM TECHNOLOGY

[1] Borys V. Uspenskyi
Uspensky.kubes@gmail.com
ORCID: 0000-0001-6360-7430

[1] Kostiantyn V. Avramov
kvavramov@gmail.com
ORCID: 0000-0002-8740-693X

[1, 2] Ihor I. Derevianko
dereviankoii2406@gmail.com
ORCID: 0000-0002-1477-3173

[1] A. Pidhornyi Institute of Mechanical Engineering Problems of NASU
2/10, Pozharskyi str., Kharkiv,
61046, Ukraine

[2] Yuzhnoye State Design Office,
3, Krivorizka str, Dnipro, 49008, Ukraine

Presented is a model of the dynamic deformation of a three-layer cylindrical shell with a honeycomb core, manufactured by fused deposition modeling (FDM), and skins reinforced with oriented carbon nano-tubes (CNT). A ULTEM 9085 thermoplastic-based honeycomb core is considered. To analyze the stress-strain state of the honeycomb core, a finite element homogenization procedure was used. As a result of this procedure, the dynamic response of the honeycomb core is modeled by a homogeneous orthotropic material, whose mechanical properties correspond to those of the core. The proposed model is based on the high-order theory, extended for the analysis of sandwich structures. The skin displacement projections are expanded along the transverse coordinate up to quadratic terms. The honeycomb core displacement projections are expanded along the transverse coordinate up to cubic terms. To ensure the integrity of the structure, shell displacement continuity conditions at the junction of the layers are used. The investigation of linear vibrations of the shell is carried out using the Rayleigh-Ritz method. For its application, the potential and kinetic energies of the structure are derived. Considered are the natural frequencies and modes of vibrations of a one-side clamped cylindrical sandwich shell. The dependence of the forms and frequencies of vibrations on the honeycomb core thickness and the direction of reinforcement of the shell skins have been investigated. It was found that the eigenforms of a sandwich shell are characterized by a smaller number of waves in the circumferential direction, as well as a much earlier appearance of axisymmetric forms. This means that when analyzing the resonant vibrations of a sandwich shell, it is necessary to take into account axisymmetric shapes. Changing the direction of reinforcement of the skins with CNTs makes it possible to significantly influence the frequencies of the natural vibrations of the shell, which are characterized by a nonzero number of waves in the circumferential direction. It was found that this parameter does not affect the frequencies of the axisymmetric shapes of the shell under consideration.

Keywords: *cylindrical sandwich shell, additive technologies, honeycomb core, nano-composite skin, eigenforms, axisymmetric vibration mode.*

Introduction

Multilayer thin-walled honeycomb sandwich structures are widely used to create objects with a high strength-to-weight ratio in aerospace, marine, energy and defense applications. Therefore, studies of such structures were carried out by many scientists. A whole series of works is devoted to the study of thin-walled sandwich structures in which the honeycomb core or the skins are reinforced with graphene nano-tubes. Free vibrations of double-curved sandwich panels with functionally-graded skins are considered in [1]. Nonlinear free and forced vibrations of cylindrical sandwich panels with an auxetic honeycomb core and CNT-reinforced skins are considered in [2]. Free vibrations of twisted conical sandwich panels with functionally graded graphene-reinforced skins and a homogeneous honeycomb core were studied in [3]. An analysis of the buckling of a sandwich plate with a honeycomb core and nano-composite skins is described in [4].

There are works in which vibrations of cylindrical composite-skin sandwich shells are considered. In [5], Flyugge's theory is used to analyze the dynamics of a thin-walled cylindrical sandwich shell. Nonlinear vibrations of cylindrical composite auxetic sandwich panels are considered in [6]. The study of various vibration properties of thin-walled sandwich structures is given in [7–11].

In [12], an extended high-order theory was proposed for the analysis of free vibrations of a sandwich plate. In it, the vibrations of each structural layer are described by a separate system of five independent functions. The honeycomb-core displacement projections are described by polynomials up to the third power along the transverse coordinate of this layer.

In this paper, this theory, described in [12], is applied to study the vibrations of three-layer cylindrical shells. The displacements of each layer of a cylindrical sandwich shell are described by its own set of variables, which consists of three projections of displacements and two angles of rotation of the normal to the median surface of the layer. Thus, the basic unknowns include fifteen variables. The skin displacement projections are expanded along the transverse coordinate up to quadratic terms. The honeycomb-core displacement projections are expanded along the transverse coordinate up to cubic terms. The Rayleigh-Ritz method is used to study the linear vibrations of the shell. The properties of linear vibrations of cylindrical sandwich shells are investigated using numerical simulation.

Formulation of the Problem

We consider a three-layer cylindrical sandwich-shell (Fig. 1) of length L with an inner radius R. The middle layer of the cylindrical shell is a honeycomb core made using FDM technology. A sketch of one honeycomb core cell and its geometric dimensions are shown in figure 2. The honeycomb core consists of regular hexagons. The outer and inner sides of the shell have the upper and lower CNT-reinforced composite skins attached thereto. The thicknesses of the shell layers (outer, median and inner) are denoted by h_t, h_c, h_b. Hereinafter, the subscript t corresponds to the outer skin; the subscript c, to the honeycomb core layer; and the subscript b, to the inner shell skin. The joints between the layers of the structure are assumed to be absolutely rigid.

To describe the stress-strain state of a three-layer structure, we will use a cylindrical coordinate system. We denote the longitudinal and circumferential coordinates of the shell by x and φ (Fig. 1). For the outer, middle and inner layers of the shell, we introduce our local transverse coordinates z_t, z_c, z_b, respectively. Thus, a three-layer cylindrical shell is analyzed in three cylindrical coordinate systems (x, φ, z_i); $i=t, c, b$. Each layer is studied in its own coordinate system.

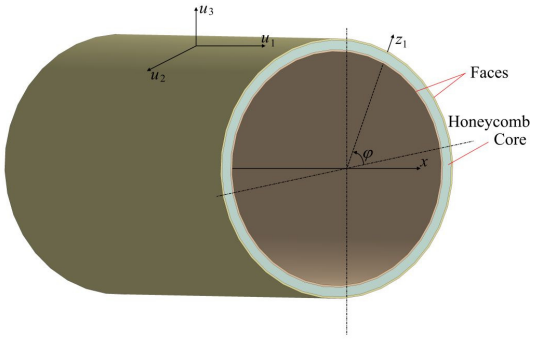

Fig. 1. Sketch of a three-layer cylindrical shell

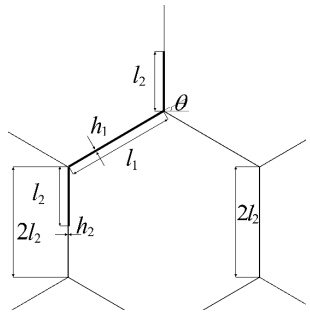

Fig. 2. Sketch of a honeycomb core cell

This article examines the linear vibrations of a three-layer cylindrical shell. The relationship between stresses and strains is linear, and is described by Hooke's law. Deformations and displacements are small, and the relationship between them is linear.

To study the vibrations of the shell, the honeycomb core is replaced with an equivalent homogeneous orthotropic layer whose parameters are calculated using the homogenization procedure for an elastic honeycomb core. Various approaches to this procedure are described in [13, 14]. Hooke's law for a homogeneous orthotropic material has the form

$$\begin{bmatrix} \sigma^{(c)}_{xx} \\ \sigma^{(c)}_{\varphi\varphi} \\ \sigma^{(c)}_{zz} \\ \sigma^{(c)}_{\varphi z} \\ \sigma^{(c)}_{xz} \\ \sigma^{(c)}_{x\varphi} \end{bmatrix} = \begin{bmatrix} C_{11} & C_{12} & C_{13} & 0 & 0 & 0 \\ C_{21} & C_{22} & C_{23} & 0 & 0 & 0 \\ C_{31} & C_{32} & C_{33} & 0 & 0 & 0 \\ 0 & 0 & 0 & C_{44} & 0 & 0 \\ 0 & 0 & 0 & 0 & C_{55} & 0 \\ 0 & 0 & 0 & 0 & 0 & C_{66} \end{bmatrix} \begin{bmatrix} \varepsilon^{(c)}_{xx} \\ \varepsilon^{(c)}_{\varphi\varphi} \\ \varepsilon^{(c)}_{zz} \\ 2\varepsilon^{(c)}_{\varphi z} \\ 2\varepsilon^{(c)}_{xz} \\ 2\varepsilon^{(c)}_{x\varphi} \end{bmatrix}, \quad (1)$$

where $\sigma^{(c)}_{xx}$, $\sigma^{(c)}_{\varphi\varphi}$, $\sigma^{(c)}_{zz}$, $\sigma^{(c)}_{\varphi z}$, $\sigma^{(c)}_{xz}$, $\sigma^{(c)}_{x\varphi}$ are stress tensor components; $\sigma^{(c)}_{xx}$, $\varepsilon^{(c)}_{\varphi\varphi}$, $\varepsilon^{(c)}_{zz}$, $\varepsilon^{(c)}_{\varphi z}$, $\varepsilon^{(c)}_{xz}$, $\varepsilon^{(c)}_{x\varphi}$ are strain tensor components. The components of the elastic matrix C_{11}, C_{12},… were obtained using the FEA-based homogenization procedure for the honeycomb core described in [13].

Let us consider the properties of a composite, which is a CNT-reinforced matrix, of which the skins of the shell under study are made. The CNTs are considered to be located along the x coordinate lines. In this paper, we consider a nano-composite with a uniform through-the-thickness CNT distribution. The volume fraction of the CNTs in the composite is denoted by V^*_{CNT}.

The mechanical properties of a nano-composite material can be calculated using the extended mixing rule [15, 16]

$$E_{11}(z)=\eta_1 V_{CNT}(z)E^{CNT}{}_{11}+V_m(z)E^m; \quad E_{22}(z)=\frac{\eta_2 E^{CNT}{}_{22}E^m}{V_{CNT}(z)E^m+V_m(z)E^{CNT}{}_{22}};$$

$$G_{12}(z)=\frac{\eta_3 G^{CNT}{}_{12}G^m}{V_{CNT}(z)G^m+V_m(z)G^{CNT}{}_{12}}; \quad \nu_{12}(z)=V_{CNT}(z)\nu^{CNT}{}_{12}+V_m(z)\nu^m;$$

$$\nu_{21}(z)=\nu_{12}(z)E_{22}(z)/E_{11}(z); \quad \rho(z)=V_{CNT}(z)\rho^{CNT}+V_m(z)\rho^m;\ V_m(z)=1-V_{CNT}(z),$$

where $E^{CNT}{}_{11}$, $E^{CNT}{}_{22}$, $G^{CNT}{}_{12}$ are Young's moduli and the shear modulus for CNTs; $\nu^{CNT}{}_{12}$ is Poisson's ratio of CNTs; η_1, η_2, η_3 are nano-reinforcement efficiency parameters; E^m, G^m are Young's modulus and the matrix-substance shear modulus; ρ^{CNT}, ρ^m are CNT and matrix densities.

To take into account the shear deformations of the skins, the nanocomposite shear moduli are taken to be the following [17] $G_{13}(z)=G_{12}(z)$; $G_{23}(z)=G_{12}(z)$. Hooke's law for the skins has the form

$$\begin{bmatrix} \sigma_{xx} \\ \sigma_{\varphi\varphi} \end{bmatrix} = \begin{bmatrix} Q_{11}(z) & Q_{12}(z) \\ Q_{12}(z) & Q_{22}(z) \end{bmatrix} \begin{bmatrix} \varepsilon_{xx} \\ \varepsilon_{\varphi\varphi} \end{bmatrix};$$

$$\sigma_{\varphi z}=G_{23}(z)\varepsilon_{\varphi z};\ \sigma_{xz}=G_{13}(z)\varepsilon_{xz};\ \sigma_{x\varphi}=G_{12}(z)\varepsilon_{x\varphi},$$

where

$$Q_{11}(z)=\frac{E_{11}(z)}{1-\nu_{12}(z)\nu_{21}(z)}; \quad Q_{22}(z)=\frac{E_{22}(z)}{1-\nu_{12}(z)\nu_{21}(z)}; \quad Q_{12}(z)=\frac{\nu_{21}(z)E_{11}(z)}{1-\nu_{12}(z)\nu_{21}(z)};$$

$\varepsilon_{x\varphi}$, $\varepsilon_{\varphi z}$, ε_{xz} are shear deformations; ε_{xx}, $\varepsilon_{\varphi\varphi}$, $\varepsilon_{\varphi z}$, ε_{xz}, $\varepsilon_{x\varphi}$ are deformation tensor components; $\sigma_{x\varphi}$, $\sigma_{\varphi z}$, σ_{xz} are shear stresses; σ_{xx}, $\sigma_{\varphi\varphi}$, $\sigma_{\varphi z}$, σ_{xz}, $\sigma_{x\varphi}$ are stress tensor components.

Stress-Strain State of a Sandwich Shell

To study the linear vibrations of structures, the Rayleigh-Ritz method is used. To apply this method, it is necessary to consider the dynamic deformation of the plate and derive the kinetic and potential energies of the structure.

The displacement projections of the points of the i-th layer of the structure onto the coordinate lines (x, φ, z_i) are denoted by $u^{(i)}{}_1(x, \varphi, z_i, \tau)$, $u^{(i)}{}_2(x, \varphi, z_i, \tau)$, $u^{(i)}{}_3(x, \varphi, z_i, \tau)$, $i=\{t, c, b\}$, where τ is time. The displacement projections of the outer and inner skins take the following form:

$$u^{(i)}{}_1(x, \varphi, z_i, \tau)=u^{(i)}(x, \varphi, \tau)+z_i\varphi^{(i)}{}_{1,1}(x, \varphi, \tau)+z_i^2\varphi^{(i)}{}_{1,2}(x, \varphi, \tau);$$
$$u^{(i)}{}_2(x, \varphi, z_i, \tau)=v^{(i)}(x, \varphi, \tau)+z_i\varphi^{(i)}{}_{2,1}(x, \varphi, \tau)+z_i^2\varphi^{(i)}{}_{2,2}(x, \varphi, \tau); \quad (2)$$
$$u^{(i)}{}_3(x, \varphi, z_i, \tau)=w^{(i)}(x, \varphi, \tau),\ i=\{t, b\},$$

where $u^{(i)}$, $v^{(i)}$, $w^{(i)}$, $i=\{t, b\}$ are the displacement projections of the middle surface onto the coordinate lines (x, φ, z_i); $\varphi^{(i)}{}_{1,1}$, $\varphi^{(i)}{}_{2,1}$, $i=\{t, b\}$ are the angles of rotation of the normal to the median surface. The functions $\varphi^{(i)}{}_{1,2}$, $\varphi^{(i)}{}_{2,2}$ are determined from the boundary conditions, which are considered below.

The displacement projections of the honeycomb core are decomposed in powers of z_c as follows:

$$u^{(c)}{}_1(x, \varphi, z_c, \tau)=u^{(c)}(x, \varphi, \tau)+z_c\varphi^{(c)}{}_{1,1}(x, \varphi, \tau)+z_c^2\varphi^{(c)}{}_{1,2}(x, \varphi, \tau)+z_c^3\varphi^{(c)}{}_{1,3}(x, \varphi, \tau);$$
$$u^{(c)}{}_2(x, \varphi, z_c, \tau)=v^{(c)}(x, \varphi, \tau)+z_c\varphi^{(c)}{}_{2,1}(x, \varphi, \tau)+z_c^2\varphi^{(c)}{}_{2,2}(x, \varphi, \tau)+z_c^3\varphi^{(c)}{}_{2,3}(x, \varphi, \tau); \quad (3)$$
$$u^{(c)}{}_3(x, \varphi, z_c, \tau)=w^{(c)}(x, \varphi, \tau)+z_c\varphi^{(c)}{}_{3,1}(x, \varphi, \tau)+z_c^2\varphi^{(c)}{}_{3,2}(x, \varphi, \tau),$$

where $u^{(c)}$, $v^{(c)}$, $w^{(c)}$ are the displacement projections of the middle surface of the honeycomb core; $\varphi^{(c)}{}_{1,1}$, $\varphi^{(c)}{}_{2,1}$ are the angles of rotation of the normal to the median surface. The functions $\varphi^{(c)}{}_{1,2}$, $\varphi^{(c)}{}_{2,2}$, $\varphi^{(c)}{}_{3,2}$, $\varphi^{(c)}{}_{1,3}$, $\varphi^{(c)}{}_{2,3}$, $\varphi^{(c)}{}_{3,1}$ are determined from the displacement continuity conditions, which are considered below.

Thus, the stress-strain state of a structure is described by fifteen functions

$$u^{(i)}(x, \varphi, \tau),\ v^{(i)}(x, \varphi, \tau),\ w^{(i)}(x, \varphi, \tau),\ \varphi^{(i)}{}_{1,1}(x, \varphi, \tau),\ \varphi^{(i)}{}_{2,1}(x, \varphi, \tau),\ i=\{t, b, c\}. \quad (4)$$

The relationship between deformations and displacements of the shell layers is presented as follows [18]:

$$\varepsilon^{(i)}{}_{xx}=\frac{\partial u^{(i)}{}_1}{\partial x};\ \varepsilon^{(i)}{}_{\varphi\varphi}=\frac{1}{1+\frac{z_i}{R_i}}\left(\frac{1}{R_i}\frac{\partial u^{(i)}{}_2}{\partial \varphi}+\frac{u^{(i)}{}_3}{R_i}\right);\ \varepsilon^{(i)}{}_{zz}=\frac{\partial u^{(i)}{}_3}{\partial z_i};$$

$$\varepsilon^{(i)}{}_{\varphi z}=\frac{\partial u^{(i)}{}_2}{\partial z_i}+\frac{1}{R_i\left(1+\frac{z_i}{R_i}\right)}\left(\frac{\partial u^{(i)}{}_3}{\partial \varphi}-u^{(i)}{}_2\right);\ \varepsilon^{(i)}{}_{xz}=\frac{\partial u^{(i)}{}_1}{\partial z_i}+\frac{\partial u^{(i)}{}_3}{\partial x};$$

$$\varepsilon^{(i)}{}_{\varphi z}=\frac{\partial u^{(i)}{}_2}{\partial x}+\frac{1}{R_i\left(1+\frac{z_i}{R_i}\right)}\frac{\partial u^{(i)}{}_1}{\partial \varphi},\ i=\{t, c, b\},$$

where the radii of the median surfaces of the layers are determined as follows:

$$R_b=R+h_b/2;\quad R_c=R+h_b+h_c/2;\quad R_t=R+h_b+h_c+h_t/2.$$

To calculate the terms of expansions (2), we use the boundary conditions [18]

$$\sigma^{(t)}{}_{xz}(x, \varphi, h_t/2, \tau)=\sigma^{(t)}{}_{\varphi z}(x, \varphi, h_t/2, \tau)=0;\ \sigma^{(b)}{}_{xz}(x, \varphi, -h_b/2, \tau)=\sigma^{(b)}{}_{\varphi z}(x, \varphi, -h_b/2, \tau)=0. \quad (5)$$

The displacement continuity conditions at the points, where the honeycomb core and the skins are connected, are as follows:

$$u^{(t)}{}_i(x, \varphi, -h_t/2, \tau)=u^{(c)}{}_i(x, \varphi, h_c/2, \tau),\ i=\{1, 2, 3\};$$
$$u^{(b)}{}_i(x, \varphi, h_b/2, \tau)=u^{(c)}{}_i(x, \varphi, -h_c/2, \tau),\ i=\{1, 2, 3\}. \quad (6)$$

Substitution of (2), (3) into (6) and (5) allows expressing expansions (2), (3) in terms of the sought-for functions (4). Then the strain tensor components can be represented in the following form:

$$\varepsilon^{(j)}{}_{xx}=\varepsilon^{(j)}{}_{xx,0}+z_jk^{(j)}{}_{xx,0}+z_j^2k^{(j)}{}_{xx,1}+z_j^3k^{(j)}{}_{xx,2};$$
$$\varepsilon^{(j)}{}_{\varphi\varphi}=\varepsilon^{(j)}{}_{\varphi\varphi,0}+z_jk^{(j)}{}_{\varphi\varphi,0}+z_j^2k^{(j)}{}_{\varphi\varphi,1}+z_j^3k^{(j)}{}_{\varphi\varphi,2};$$
$$\varepsilon^{(j)}{}_{x\varphi}=\varepsilon^{(j)}{}_{x\varphi,0}+z_jk^{(j)}{}_{x\varphi,0}+z_j^2k^{(j)}{}_{x\varphi,1}+z_j^3k^{(j)}{}_{x\varphi,2};$$
$$\varepsilon^{(j)}{}_{xz}=\varepsilon^{(j)}{}_{xz,0}+z_jk^{(j)}{}_{xz,0}+z_j^2k^{(j)}{}_{xz,1}+z_j^3k^{(j)}{}_{xz,2}; \quad (7)$$
$$\varepsilon^{(j)}{}_{\varphi z}=\varepsilon^{(j)}{}_{\varphi z,0}+z_jk^{(j)}{}_{\varphi z,0}+z_j^2k^{(j)}{}_{\varphi z,1}+z_j^3k^{(j)}{}_{\varphi z,2};\quad j=\{t, b, c\};$$
$$\varepsilon^{(c)}{}_{zz}=\varepsilon^{(c)}{}_{zz,0}+z_ck^{(c)}{}_{zz,0},$$

where the coefficients of expansion in z_j, $j=\{t, b, c\}$ are linear functions of variables (4), and their partial derivatives with respect to x and φ.

The kinetic energy of a three-layer structure is represented as the sum of the kinetic energies of each of the layers separately

$$T=\frac{1}{2}\sum_{i=\{t,c,b\}}\int_0^L\int_0^{2\pi}\int_{-\frac{h_i}{2}}^{\frac{h_i}{2}}\rho_i(z_i)\left(\left(\dot{u}^{(i)}{}_1\right)^2+\left(\dot{u}^{(i)}{}_2\right)^2+\left(\dot{u}^{(i)}{}_3\right)^2\right)(R_i+z_i)dz_i d\varphi dx,$$

where the dot means the derivative with respect to time; $\rho_i(z_i)$ is the density of the i-th layer.

After integration over z_i,, the kinetic energy of the entire structure takes the form

$$T=\frac{1}{2}\sum_{i=\{t,b\}}\int_0^L\int_0^{2\pi}\sum_{k=0}^{4}\left(r^{(i)}{}_k T^{(i)}{}_k\right)d\varphi dx+\frac{1}{2}\int_0^L\int_0^{2\pi}\left(T^{(c)}{}_0+T^{(c)}{}_2+T^{(c)}{}_4\right)d\varphi dx, \tag{8}$$

where $r^{(i)}{}_j=\int_{-\frac{h_i}{2}}^{\frac{h_i}{2}} z_i{}^j\rho_i(z_i)dz_i$, $i=\{t, b\}$; $T^{(i)}{}_k$, $i=\{t, b\}$, $k=0\ldots4$, $T^{(c)}{}_k$, $k=\{2, 4, 6\}$ are the quadratic forms of the time derivatives of functions (4) and their partial derivatives with respect to x and φ.

We represent the potential energy of the middle layer in the following form:

$$\Pi^{(c)}=\frac{1}{2}\int_0^L\int_0^{2\pi}\int_{-\frac{h_c}{2}}^{\frac{h_c}{2}}(\sigma^{(c)}{}_{xx}\varepsilon^{(c)}{}_{xx}+\sigma^{(c)}{}_{\varphi\varphi}\varepsilon^{(c)}{}_{\varphi\varphi}+\sigma^{(c)}{}_{zz}\varepsilon^{(c)}{}_{zz}+2\sigma^{(c)}{}_{x\varphi}\varepsilon^{(c)}{}_{x\varphi}+$$
$$+2\sigma^{(c)}{}_{\varphi z}\varepsilon^{(c)}{}_{\varphi z}+2\sigma^{(c)}{}_{xz}\varepsilon^{(c)}{}_{xz})(R_c+z_c)dz_c d\varphi dx\ . \tag{9}$$

In expression (9), we take into account Hooke's law (1) and (7). After integration over z_c, the potential energy is represented as

$$\Pi^{(c)}=\frac{1}{2}\int_0^L\int_0^{2\pi}(\Pi^{(c)}{}_0+\Pi^{(c)}{}_2+\Pi^{(c)}{}_4)d\varphi dx,$$

where $\Pi^{(c)}{}_k$, $k=\{2, 4, 6\}$ are the quadratic forms of the coefficients of expansions (7).

Likewise, the potential energy of the skins is represented as follows:

$$\Pi^{(i)}=\frac{1}{2}\int_0^L\int_0^{2\pi}\int_{-\frac{h_i}{2}}^{\frac{h_i}{2}}(\sigma^{(i)}{}_{xx}\varepsilon^{(i)}{}_{xx}+\sigma^{(i)}{}_{\varphi\varphi}\varepsilon^{(i)}{}_{\varphi\varphi}+\sigma^{(i)}{}_{x\varphi}\varepsilon^{(i)}{}_{x\varphi}+\sigma^{(i)}{}_{\varphi z}\varepsilon^{(i)}{}_{\varphi z}+\sigma^{(i)}{}_{xz}\varepsilon^{(i)}{}_{xz})(R_i+z_i)dz_i d\varphi dx=$$

$$=\frac{1}{2}\int_0^L\int_0^{2\pi}\int_{-\frac{h_i}{2}}^{\frac{h_i}{2}}(Q_{11}\left(\varepsilon^{(i)}{}_{xx}\right)^2+2Q_{12}\varepsilon^{(i)}{}_{\varphi\varphi}\varepsilon^{(i)}{}_{xx}+Q_{22}\left(\varepsilon^{(i)}{}_{\varphi\varphi}\right)^2+G_{23}\left(\varepsilon^{(i)}{}_{\varphi z}\right)^2+ \tag{10}$$
$$+G_{13}\left(\varepsilon^{(i)}{}_{xz}\right)^2+G_{12}\left(\varepsilon^{(i)}{}_{x\varphi}\right)^2)\left(R_i+z_i\right)dz_i d\varphi dx,\ i=\{t, b\}.$$

Let us integrate (10) over z_i. Then we represent the potential energy in the following form:

$$\Pi^{(i)}=\frac{1}{2}\int_0^L\int_0^{2\pi}\sum_{j=0}^{4}\Pi^{(i)}{}_j(x,\varphi)R_i d\varphi dx,\ i=\{t, b\},$$

where $\Pi^{(i)}{}_j$, $i=\{t, b\}$, $j=0\ldots4$ are the quadratic forms of functions (4) and their partial derivatives with respect to x and φ.

The potential energy of the structure is equal to the sum of the potential energies of its three layers

$$\Pi=\Pi^{(t)}+\Pi^{(c)}+\Pi^{(b)}. \tag{11}$$

Further, we consider cantilever cylindrical shells that are clamped at x=0. On the clamped side, geometric boundary conditions are satisfied, and on the free side, only force boundary conditions are satisfied. Since the further analysis uses the Rayleigh-Ritz method, only geometric boundary conditions are taken into account, which take the following form:

$$u^{(i)}|_{x=0}=v^{(i)}|_{x=0}=w^{(i)}|_{x=0}=\varphi^{(i)}{}_{1,1}|_{x=0}=\varphi^{(i)}{}_{2,1}|_{x=0}=0;\ i=\{t, c, b\}. \tag{12}$$

Free Vibrations of a Cylindrical Sandwich Shell

The linear vibrations of the structure are investigated using the Rayleigh-Ritz method. The displacement projections of the median surface and the angles of rotation of the normal thereto are expressed as follows:

$$\begin{bmatrix} u^{(i)} \\ v^{(i)} \\ w^{(i)} \\ \varphi^{(i)}{}_{1,1} \\ \varphi^{(i)}{}_{2,1} \end{bmatrix} = \begin{bmatrix} U_i(x,\varphi) \\ V_i(x,\varphi) \\ W_i(x,\varphi) \\ \Phi_i(x,\varphi) \\ \Psi_i(x,\varphi) \end{bmatrix} \cos(\omega\tau),\ i=\{t, c, b\}, \tag{13}$$

where ω is the frequency of natural vibrations; $U_i(x, \varphi)$, $V_i(x, \varphi)$, $W_i(x, \varphi)$, $\Phi_i(x, \varphi)$, $\Psi_i(x, \varphi)$ are the functions that satisfy boundary conditions (12). We represent these functions in the form

$$U_i = \cos(n\varphi)\sum_{m=1}^{N^{(i)}{}_u} U^{(i)}{}_m F^{(u)}{}_m(x);\ V_i = \sin(n\varphi)\sum_{m=1}^{N^{(i)}{}_v} V^{(i)}{}_m F^{(v)}{}_m(x);\ W_i = \cos(n\varphi)\sum_{m=1}^{N^{(i)}{}_w} W^{(i)}{}_m F^{(w)}{}_m(x);$$

$$\Phi_i = \cos(n\varphi)\sum_{m=1}^{N^{(i)}{}_\Phi} \Phi^{(i)}{}_m F^{(\Phi)}{}_m(x);\quad \Psi_i = \sin(n\varphi)\sum_{m=1}^{N^{(i)}{}_\Psi} \Psi^{(i)}{}_m F^{(\Psi)}{}_m(x),\ i=\{t, c, b\}, \tag{14}$$

where $F^{(u)}{}_m(x)$, $F^{(v)}{}_m(x)$, $F^{(w)}{}_m(x)$, $F^{(\Phi)}{}_m(x)$, $F^{(\Psi)}{}_m(x)$ are the basis functions satisfying boundary conditions (12); n is the number of waves in the circumferential direction. We represent the unknown expansion coefficients $U^{(i)}{}_m$, $V^{(i)}{}_m$, $W^{(i)}{}_m$, $\Phi^{(i)}{}_m$, $\Psi^{(i)}{}_m$ as one vector of dimension N: $\mathbf{a} = (A_1,\ldots,A_N)$.

Expansions (13), (14) are introduced into the kinetic and potential energies of the structure (8), (11). After calculating the integrals in (8) and (11), the energy value can be represented in the following form:

$$T=\omega^2\sin^2(\omega\tau)T^*(\mathbf{a});\quad \Pi=\cos^2(\omega\tau)\Pi^*(\mathbf{a}). \tag{15}$$

The functions $T^*(\mathbf{a})$, $\Pi^*(\mathbf{a})$ are quadratic forms with respect to the components of the vector of unknowns **a.** The displacements of the structure deliver the minimum value of the functional

$$\int_0^{2\pi/\omega} (T-\Pi)d\tau \to \min. \tag{16}$$

We introduce representation (15) into (16) and perform integration. Then the displacement of the structure is described by the minimum of the following function:

$$\Pi^*(\mathbf{a})-\omega^2 T^*(\mathbf{a})\to\min.$$

This minimum is described by the system of equations $\frac{\partial}{\partial A_j}\left(\Pi^*(\mathbf{a})-\omega^2 T^*(\mathbf{a})\right)=0$; $j=1,2,\ldots,N$, which are reduced to the eigen-value problem:

$$\mathbf{Ka}=\omega^2\mathbf{Ma},$$

where **K**, **M** are the stiffness and mass matrices.

Numerical Analysis of Linear Vibrations

The results of calculating the linear free vibrations of a cylindrical sandwich shell with an elastic honeycomb core are discussed below.

The geometry of one honeycomb core cell is shown in figure 2. The core section is shown in figure 3. Through the homogenization procedure, the honeycomb core is replaced with a homogeneous orthotropic material. Homogenization procedures for calculating the mechanical characteristics of a material are discussed in [13, 14].

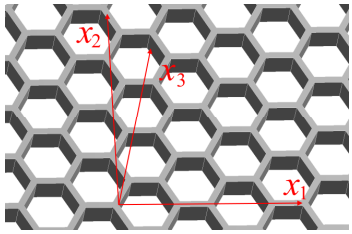

Fig. 3. Sketch of a honeycomb core fragment

Hooke's law for a homogenized honeycomb core has the form (1). A honeycomb core made of the ULTEM 9085 plastic using FDM technology is considered. The honeycomb cores are printed using FDM technology so that the filament runs along the honeycomb cell wall. Its geometrical parameters are as follows: l_1=6.0476 mm; l_2=3.0238 mm; h=0.5 mm; $h_2=h_1=h$; h_c=10–20 mm; θ=60°.

The mechanical properties of parts printed using FDM technology are divided according to three orthogonal directions: the direction of filament deposition by the extruder, the direction orthogonal to the layers deposited, and the direction perpendicular to the previous two. The mechanical properties of ULTEM 9085 were determined experimentally. The experimental analysis results are presented in article [19]. The mechanical properties of ULTEM 9085 are as follows:

$$E_{11}=2.25 \text{ GPa}; E_{22}=2.96 \text{ GPa}; E_{33}=2.41 \text{ GPa}; \nu_{12}=0.31;$$
$$\nu_{23}=0.26; \nu_{13}=0.33; G_{12}=667 \text{ MPa}; G_{23}=889 \text{ MPa}; G_{13}=829 \text{ MPa}; \quad (17)$$

material density $\rho=1267$ kg/m^3. It follows from (17) that the material is weakly orthotropic. "1" refers to the filament deposition direction; "2" refers to the direction perpendicular to "1" in the plane of the layer; "3" refers to the direction of interlayer interaction.

Using the homogenization procedure described in [13], the following estimates of the effective mechanical properties of the honeycomb core were obtained: $E_{xx}=2.907$ MPa; $E_{\varphi\varphi}=2.907$ MPa; $E_{zz}=214.6$ MPa; $G_{x\varphi}=1.118$ MPa; $G_{xz}=39.116$ MPa; $G_{\varphi z}=39.162$ MPa; $\nu_{x\varphi}=0.973$; $\nu_{xz}=0.005$; $\nu_{\varphi z}=0.004$.

The skins of the sandwich shell are made of a composite, which is a CNT-reinforced PmPV matrix. The volumetric part of the CNTs in the composite is $V^*_{CNT}=0.28$. The values of reinforcement efficiency parameters for this combination of the matrix and CNTs $\eta_1=0.141$; $\eta_2=1.585$; $\eta_3=1.109$. The numerical values of the mechanical properties of the CNTs and nano-composite matrix are as follows [20]: $E^{CNT}{}_{11}=5.6466$ TPa; $E^{CNT}{}_{22}=7.08$ TPa; $G^{CNT}{}_{12}=G^{CNT}{}_{13}=1.9445$ TPa; $G^{CNT}{}_{23}=2.3334$ TPa; $\nu^{CNT}{}_{12}=0.175$; $\rho^{CNT}=1400$ kg/m^3; $E^m=2.5$ GPa; $\nu^m=0.34$; $\rho^m=1{,}150$ kg/m^3.

The cylindrical sandwich shell (Fig. 1) has the following geometrical parameters: $L=1$ m; $R=0.25$ m; $h_t=h_b=1$ mm. Two options for the thickness of the honeycomb core were considered: $h_c=10$ mm and $h_c=20$ mm. In the shell skins, the CNTs are distributed uniformly through the thickness. When calculating free vibrations in expansions (14), we took the same number of terms $N^{(i)}{}_u=N^{(i)}{}_v=N^{(i)}{}_w=N^{(i)}{}_\Phi=N^{(i)}{}_\Psi=N_x$, $i=t, c, b$. To analyze the convergence of the natural frequencies, calculations were performed with a different number of terms in expansions (14): $N_x=15$, $N_x=25$, $N_x=35$. The results obtained were compared with the data of finite element modeling in the ANSYS software package.

The basis functions in expansions (14), satisfying the boundary conditions (12), were chosen in the following form:

$$F^{(u)}{}_m(x)=F^{(v)}{}_m(x)=F^{(w)}{}_m(x)=F^{(\Phi)}{}_m(x)=F^{(\Psi)}{}_m(x)=\sin((2m-1)\pi x/(2L)).$$

The results of the analysis of the natural vibration frequencies are given in tables 1, 2. They represent the natural frequencies (Hz) of a three-layer structure with different honeycomb core thicknesses. The first columns of these tables show the number of waves in the circumferential direction. The second column presents the results of calculating the natural frequencies in the ANSYS software package. The third, fifth, and seventh columns show the natural frequencies obtained by the Rayleigh-Ritz method with a different number of basis functions in expansions (14). The fourth, sixth and eighth columns give the relative difference between the results obtained by the Rayleigh-Ritz method and the finite element method (in percent).

With an increase in the number of terms in expansions (14), the natural frequencies obtained by the Rayleigh-Ritz method decrease, approaching the natural frequencies obtained by the finite element method. The natural frequencies obtained by the two methods are close. The maximum relative difference of the natural frequencies obtained by the two methods is 3.85%. As follows from tables 1 and 2, the spectrum of the natural frequencies is very dense. The lowest natural frequencies are observed at a small number of waves in the circumferential direction n. In all the cases under consideration, the first natural frequency is observed at $n=2$. In isotropic cylindrical shells, this number is slightly higher ($n=4$) [18].

As the thickness of the honeycomb core increases, the shell becomes harder. This leads to an increase in the natural frequencies.

The first four natural modes of vibrations of a cylindrical sandwich shell with a honeycomb core thickness $h_c=20$ mm are shown in figure 4. These modes correspond to the first four natural frequencies in table 2. The mode of vibrations (Fig. 4, c) is axisymmetric. Its natural frequency is not a multiple. All other modes of vibrations shown in figure 4 have conjugate forms.

Table 1. The results of calculating the natural frequencies in Hz at h_c=10 mm

n	ANSYS	N_x=15	δ, %	N_x=25	δ, %	N_x=35	δ, %
2	123.4	125.6	1.78	125.2	1.46	125.1	1.38
1	161.0	161.5	0.31	161.3	0.19	161.2	0.12
3	189.3	196.4	3.75	196.2	3.65	196.1	3.59
0	224.8	224.8	0.00	224.8	0.00	224.8	0.00
3	313.2	323.5	3.29	321.0	2.49	320.1	2.20
4	324.7	337.1	3.82	336.3	3.57	335.5	3.33
2	332.4	338.6	1.87	337.0	1.38	336.9	1.35
4	395.2	410.4	3.85	408.4	3.34	407.7	3.16
1	471.3	475.5	0.89	474.2	0.62	473.8	0.53
5	496.8	514.6	3.58	514.4	3.54	514.4	3.54

Table 2. The results of calculating the natural frequencies in Hz at h_c=20 mm

n	ANSYS	N_x=15	δ, %	N_x=25	δ, %	N_x=35	δ, %
2	142.7	146.3	2.52	145.9	2.24	145.8	2.17
1	145.4	146.0	0.41	145.7	0.21	145.6	0.14
0	196.5	196.5	0.00	196.5	0.00	196.5	0.00
3	278.3	288.3	3.59	288.0	3.49	287.9	3.45
2	339.9	347.2	2.15	344.8	1.44	343.8	1.15
3	391.2	403.8	3.22	401.5	2.63	400.6	2.40
1	430.7	435.0	1.00	433.6	0.67	433.0	0.53
4	484.5	500.4	3.28	500.2	3.24	500.2	3.24
4	552.3	571.0	3.39	569.4	3.10	568.8	2.99
0	589.2	589.2	0.00	589.2	0.00	589.2	0.00

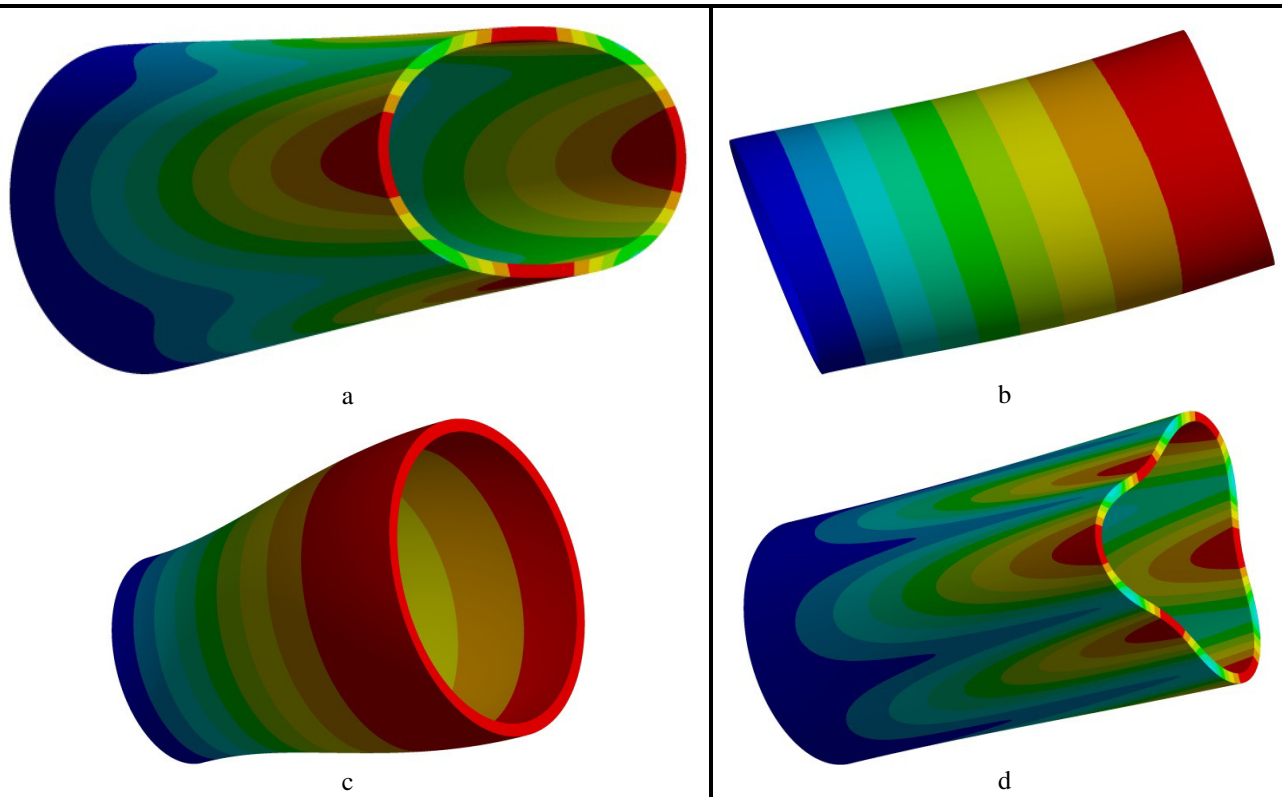

Fig. 4. The first four natural modes of vibrations:
a – *n*=2; b – *n*=1; c – *n*=0; d – *n*=3

Note that among the natural modes of vibrations of a shell with a honeycomb core, the axisymmetric mode of vibration (n=0) arises much earlier than in a single-layer orthotropic shell. This fact must be taken into account when studying the resonant vibrations of sandwich shells.

Let us consider the dependence of the natural vibration frequencies of the structure when the orientation of the CNTs, which are used to reinforce the shell skins, is changed. Let us introduce the angles of skin reinforcement. Since all CNTs are oriented in the same way, one angle is sufficient for each skin to determine the direction of reinforcement. The angle of reinforcement of the outer skin will be denoted by $\beta^{(t)}$, and that of the inner one, by $\beta^{(b)}$. If $\beta^{(i)}=0$; $i=t, b$, then the CNTs are located along the x axis (Fig. 1). If $\beta^{(i)}=\pi/2$; $i=t, b$, then the CNTs are located along the φ axis.

The results of calculating the natural frequencies of a shell with a honeycomb core thickness h_c=20 mm are given in table 3. The first column of the table shows the natural frequency number. The second, fourth and sixth columns show the natural frequencies in Hz for different values of the skin reinforcement angles. The number of waves in the circumferential direction n is recorded in the third, fifth and seventh columns of the table.

The CNT orientation sufficiently affects the natural frequencies, characterized the $n\neq0$ value.

Table 3. Natural frequencies of the sandwich shell (Hz) with different CNT orientations in the skins

Frequency No.	$\beta^{(t)}=\beta^{(b)}=0$	n	$\beta^{(t)}=0$; $\beta^{(b)}=\pi/2$	n	$\beta^{(t)}=\pi/2$; $\beta^{(b)}=0$	n
1	145.7	1	143.3	1	134.0	1
2	145.9	2	170.5	2	158.8	2
3	196.5	0	196.5	0	196.5	0
4	288.0	3	323.4	2	291.0	2
5	344.8	2	377.0	3	353.9	3
6	401.5	3	431.4	1	399.3	3
7	433.6	1	440.1	3	404.6	1
8	500.2	4	527.5	2	487.8	2
9	569.4	4	563.7	3	514.4	3
10	589.2	0	589.2	0	589.2	0

Conclusions

A model of dynamic deformation of a cylindrical sandwich shell with a honeycomb core, made using FDM technology, and nano-composite skins has been constructed. The displacements of each shell layer are described by the latter's own set of variables, which consists of the displacement projections of the median surface of the layer and the angles of rotation of the normal to the median surface. The displacement projections of the skins are expanded along the transverse coordinate up to quadratic terms. The displacement projections of the honeycomb core are expanded along the transverse coordinate up to cubic terms. To ensure the integrity of the structure, the displacement continuity conditions at the boundaries between the layers are used.

Among the natural modes of vibration of a shell with a honeycomb core, the axisymmetric mode of vibration arises much earlier than in a single-layer orthotropic shell. This fact must be taken into account when studying the resonant vibrations of sandwich shells.

The orientation of the CNTs in the shell skins can significantly affect the natural frequencies. Changing the CNT orientation can serve to detune the shell structure from resonance.

Financing

This research was supported by the National Research Foundation of Ukraine (project number 128/02/2020).

References

1. Sahu, N. K., Biswal, D. K., Joseph, S. V, & Mohanty, S. C. (2020). Vibration and damping analysis of doubly curved viscoelastic-FGM sandwich shell structures using FOSDT. *Structures*, vol. 26, pp. 24–38. https://doi.org/10.1016/j.istruc.2020.04.007.
2. Quyen, N. V., Thanh, N. V., Quan, T. Q., & Duc, N. D. (2021). Nonlinear forced vibration of sandwich cylindrical panel with negative Poisson's ratio auxetic honeycombs core and CNTRC face sheets. *Thin-Walled Structures*, vol. 162, paper 107571. https://doi.org/10.1016/j.tws.2021.107571.

3. Singha, T. D., Rout, M., Bandyopadhyay, T., & Karmakar, A. (2021). Free vibration of rotating pretwisted FG-GRC sandwich conical shells in thermal environment using HSDT. *Composite Structures*, vol. 257, paper 113144. https://doi.org/10.1016/j.compstruct.2020.113144.
4. Bacciocchi, M. & Tarantino, A. M. (2020). Critical buckling load of honeycomb sandwich panels reinforced by threephase orthotropic skins enhanced by carbon nanotubes. *Composite Structures*, vol. 237, paper 111904. https://doi.org/10.1016/j.compstruct.2020.111904.
5. Li, Y., Yao, W., & Wang, T. (2020). Free flexural vibration of thin-walled honeycomb sandwich cylindrical shells. *Thin–Walled Structures*, vol. 157, paper 107032. https://doi.org/10.1016/j.tws.2020.107032.
6. Duc, N. D., Seung-Eock, K., Tuan, N. D., Tran, P., & Khoa, N. D. (2017). New approach to study nonlinear dynamic response and vibration of sandwich composite cylindrical panels with auxetic honeycomb core layer. *Aerospace Science and Technology*, vol. 70, pp. 396–404. https://doi.org/10.1016/j.ast.2017.08.023.
7. Eipakchi, H. & Nasrekani, F. M. (2020). Vibrational behavior of composite cylindrical shells with auxetic honeycombs core layer subjected to a moving pressure. *Composite Structures*, vol. 254, paper 112847. https://doi.org/10.1016/j.compstruct.2020.112847.
8. Nath, J. K. & Das, T. (2019). Static and free vibration analysis of multilayered functionally graded shells and plates using an efficient zigzag theory. *Mechanics of Advanced Materials and Structures*, vol. 26, pp. 770–788. https://doi.org/10.1080/15376494.2017.1410915.
9. Chehreghani, M., Pazhooh, M. D., & Shakeri, M. (2019). Vibration analysis of a fluid conveying sandwich cylindrical shell with a soft core. *Composite Structures*, vol. 230, paper 111470. https://doi.org/10.1016/j.compstruct.2019.111470.
10. Yang, C., Jin, G., Liu, Z., Wang, X., & Miao, X. (2015). Vibration and damping analysis of thick sandwich cylindrical shells with a viscoelastic core under arbitrary boundary conditions. *International Journal of Mechanical Sciences*, vol. 92, pp. 162–177. https://doi.org/10.1016/j.ijmecsci.2014.12.003.
11. Karakoti, A., Pandey, S., & Kar, V. R. (2020). Free vibration response of P-FGM and S-FGM sandwich shell panels: A comparison. *Materials Today: Proceedings*, vol. 28, part 3, pp. 1701–1705. https://doi.org/10.1016/j.matpr.2020.05.131.
12. Ramian, A., Jafari-Talookolaei, R.-A., Valvo, P. S., & Abedi, M. (2020). Free vibration analysis of sandwich plates with compressible core in contact with fluid. *Thin–Walled Structures*, vol. 157, paper 107088. https://doi.org/10.1016/j.tws.2020.107088.
13. Uspenskiy, B., Avramov, K., Derevyanko, I., & Biblik, I. (2021). *K raschetu mekhanicheskikh kharakteristik sotovykh zapolniteley, izgotovlennykh additivnymi tekhnologiyami FDM* [Calculation of mechanical characteristics of honeycomb cores made by additive FDM technologies]. *Aviatsionno-kosmicheskaya tekhnika i tekhnologiya – Aerospace Engineering and Technology*, no. 1, pp. 14–20 (in Russian). https://doi.org/10.32620/aktt.2021.1.02.
14. Avramov, K. V., Uspenskyi, B. V., & Derevianko, I. I. (2021). Analytical calculation of the mechanical properties of honeycombs printed using the FDM additive manufacturing technology. *Journal of Mechanical Engineering – Problemy Mashynobuduvannia*, 2021, vol. 24, no. 2, pp. 16–23. https://doi.org/10.15407/pmach2021.02.016.
15. Shen, H. S. (2009). Nonlinear bending of functionally graded carbon nanotube-reinforced composite plates in thermal environments. *Composite Structures*, vol. 91, iss. 1, pp. 9–19. https://doi.org/10.1016/j.compstruct.2009.04.026.
16. Wang, Q., Qin, B., Shi, D., & Liang, Q. (2017). A semi-analytical method for vibration analysis of functionally graded carbon nanotube reinforced composite doubly-curved panels and shells of revolution. *Composite Structures*, vol. 174, pp. 87–109. https://doi.org/10.1016/j.compstruct.2017.04.038.
17. Wang, Q., Cui, X., Qin, B., & Liang, Q. (2017). Vibration analysis of the functionally graded carbon nanotube reinforced composite shallow shells with arbitrary boundary conditions. *Composite Structures*, vol. 182, pp. 364–379. https://doi.org/10.1016/j.compstruct.2017.09.043.
18. Amabili, M. & Reddy, J. N. (2010). A new non-linear higher-order shear deformation theory for large-amplitude vibrations of laminated doubly curved shells. *International Journal of Non-Linear Mechanics*, vol. 45, iss. 4, pp. 409–418. https://doi.org/10.1016/j.ijnonlinmec.2009.12.013.
19. Derevianko, I., Avramov, K., Uspenskyi, B., & Salenko, A. (2021). *Eksperymentalnyi analiz mekhanichnykh kharakterystyk detalei raket-nosiiv, vyhotovlenykh za dopomohoiu FDM adytyvnykh tekhnolohii* [Experimental analysis of the mechanical characteristics of the components of the carrier rockets, prepared with the help of FDM additive technologies]. *Tekhnichna mekhanika – Technical Mechanics*, no. 1, pp. 92–100. https://doi.org/10.15407/itm2021.01.092.
20. Duc, N. D., Cong, P. H., Tuan, N, D, Tran, P., & Thanh, N. V. (2017). Thermal and mechanical stability of functionally graded carbon nanotubes (FG CNT)-reinforced composite truncated conical shells surrounded by the elastic foundations. *Thin–Walled Structures*, vol. 115, pp. 300–310. https://doi.org/10.1016/j.tws.2017.02.016.

Received 13 October 2021

Коливання циліндричної сандвіч-оболонки з наповнювачем, що виготовлений за допомогою технології FDM

[1] Б. В. Успенський, [1] К. В. Аврамов, [1, 2] І. І. Деревянко

[1] Інститут проблем машинобудування ім. А. М. Підгорного НАН України,
61046, Україна, м. Харків, вул. Пожарського, 2/10

[2] Державне підприємство «Конструкторське бюро «Південне» ім. М.К. Янгеля»,
49008, Україна, м. Дніпро, вул. Криворізька, 3

Наведено модель динамічного деформування тришарової циліндричної оболонки зі стільниковим заповнювачем, який виготовлено за допомогою технології FDM, та обшивками, які армовано вуглецевими нанотрубками. Розглянуто стільниковий заповнювач, який виготовлено з термопластику ULTEM 9085. Для аналізу напружено-деформованого стану стільникового заповнювача використовується методика скінченно-елементної гомогенізації. Внаслідок цієї процедури динамічний відклик стільникового заповнювача моделюється однорідним ортотропним матеріалом, механічні властивості якого відповідають властивостям заповнювача. Запропонована модель базується на теорії високого порядку, яку розширено для аналізу сандвіч-конструкцій. Проекції переміщень обшивок оболонки розкладено за поперечною координатою до квадратичних доданків. Проєкції переміщень стільникового заповнювача розкладено за поперечною координатою до кубічних доданків. Для забезпечення цілісності конструкції використано умови безперервності переміщень оболонки на стиках шарів. Лінійні коливання оболонки досліджено за допомогою методу Релея-Рітца. Для його застосування отримано потенційну та кінетичну енергії конструкції. Розглянуто власні частоти та форми коливань циліндричної сандвіч-оболонки, яку затиснено з одного боку. Досліджено залежність форм та частот коливань оболонки від товщини стільникового заповнювача та напряму армування обшивок вуглецевими нанотрубками. Виявлено, що для власних форм сандвіч-оболонки характерною є менша кількість хвиль в окружному напрямку, а також вісесиметричні форми, що виникають набагато раніше. З цього випливає, що аналіз резонансних коливань сандвіч-оболонки слід здійснювати з урахуванням вісесиметричних форм. Зміна напрямку армування обшивок вуглецевими нанотрубками дозволяє суттєво впливати на власні частоти коливань оболонки, які характеризуються ненульовою кількістю хвиль в окружному напрямку. Встановлено, що цей параметр не впливає на частоти вісесиметричних форм розглянутої оболонки.

Ключові слова: *циліндрична сандвіч-оболонка, адитивні технології, стільниковий заповнювач, нанокомпозитна обшивка, власні форми, вісесиметрична форма коливань.*

Література

1. Sahu N. K., Biswal D. K., Joseph S. V, Mohanty S. C. Vibration and damping analysis of doubly curved viscoelastic-FGM sandwich shell structures using FOSDT. *Structures*. 2020. Vol. 26. P. 24–38. https://doi.org/10.1016/j.istruc.2020.04.007.
2. Quyen N. V., Thanh N. V., Quan T. Q., Duc N. D. Nonlinear forced vibration of sandwich cylindrical panel with negative Poisson's ratio auxetic honeycombs core and CNTRC face sheets. *Thin-Walled Structures*. 2021. Vol. 162. Paper 107571. https://doi.org/10.1016/j.tws.2021.107571.
3. Singha T. D., Rout M., Bandyopadhyay T., Karmakar A. Free vibration of rotating pretwisted FG-GRC sandwich conical shells in thermal environment using HSDT. *Composite Structures*. 2021. Vol. 257. Paper 113144. https://doi.org/10.1016/j.compstruct.2020.113144.
4. Bacciocchi M., Tarantino A. M. Critical buckling load of honeycomb sandwich panels reinforced by threephase orthotropic skins enhanced by carbon nanotubes. *Composite Structures*. 2020. Vol. 237. Paper 111904. https://doi.org/10.1016/j.compstruct.2020.111904.
5. Li Y., Yao W., Wang T. Free flexural vibration of thin-walled honeycomb sandwich cylindrical shells. *Thin–Walled Structures*. 2020. Vol. 157. Paper 107032. https://doi.org/10.1016/j.tws.2020.107032.
6. Duc N. D., Seung-Eock K., Tuan N. D., Tran P., Khoa N. D. New approach to study nonlinear dynamic response and vibration of sandwich composite cylindrical panels with auxetic honeycomb core layer. *Aerospace Sci. and Technology*. 2017. Vol. 70. P. 396–404. https://doi.org/10.1016/j.ast.2017.08.023.
7. Eipakchi H., Nasrekani F. M. Vibrational behavior of composite cylindrical shells with auxetic honeycombs core layer subjected to a moving pressure. *Composite Structures*. 2020. Vol. 254. Paper 112847. https://doi.org/10.1016/j.compstruct.2020.112847.
8. Nath J. K., Das T. Static and free vibration analysis of multilayered functionally graded shells and plates using an efficient zigzag theory. *Mech. Advanced Materials and Structures*. 2019. Vol. 26. P. 770–788. https://doi.org/10.1080/15376494.2017.1410915.

9. Chehreghani M., Pazhooh M. D., Shakeri M. Vibration Analysis of a Fluid Conveying Sandwich Cylindrical Shell with a Soft Core. *Composite Structures.* 2019. Vol. 230. Paper 111470. https://doi.org/10.1016/j.compstruct.2019.111470.
10. Yang C., Jin G., Liu Z., Wang X., Miao X. Vibration and damping analysis of thick sandwich cylindrical shells with a viscoelastic core under arbitrary boundary conditions. *Intern. J. Mech. Sci*. 2015. Vol. 92. P. 162–177. https://doi.org/10.1016/j.ijmecsci.2014.12.003.
11. Karakoti A., Pandey S., Kar V. R. Free vibration response of P-FGM and S-FGM sandwich shell panels: A comparison. *Materials Today: Proceedings*. 2020. Vol. 28. P. 1701–1705. https://doi.org/10.1016/j.matpr.2020.05.131.
12. Ramian A., Jafari-Talookolaei R.-A., Valvo P. S., Abedi M. Free vibration analysis of sandwich plates with compressible core in contact with fluid. *Thin–Walled Structures*. 2020. Vol. 157. Paper 107088. https://doi.org/10.1016/j.tws.2020.107088.
13. Успенский Б., Аврамов К., Деревянко И., Библик И. К расчету механических характеристик сотовых заполнителей, изготовленных аддитивными технологиями FDM. *Авиац.-косм. техника и технология*. 2021. Вып. 1. С. 14–20. https://doi.org/10.32620/aktt.2021.1.02.
14. Avramov K. V., Uspenskyi B. V., Derevianko I. I. Analytical calculation of the mechanical properties of honeycombs printed using the FDM additive manufacturing technology. *Journal of Mechanical Engineering – Problemy Mashynobuduvannia.* 2021. Vol. 24. No. 2. P. 16–23. https://doi.org/10.15407/pmach2020.02.014.
15. Shen H. S. Nonlinear bending of functionally graded carbon nanotube-reinforced composite plates in thermal environments. *Composite Structures*. 2009. Vol. 91. Iss. 1. P. 9–19. https://doi.org/10.1016/j.compstruct.2009.04.026.
16. Wang Q., Qin B., Shi D., Liang Q. A semi-analytical method for vibration analysis of functionally graded carbon nanotube reinforced composite doubly-curved panels and shells of revolution. *Composite Structures*. 2017. Vol. 174. P. 87–109. https://doi.org/10.1016/j.compstruct.2017.04.038.
17. Wang Q., Cui X., Qin B., Liang Q. Vibration analysis of the functionally graded carbon nanotube reinforced composite shallow shells with arbitrary boundary conditions. *Composite Structures*. 2017. Vol. 182. P. 364–379. https://doi.org/10.1016/j.compstruct. 2017.09.043.
18. Amabili M., Reddy J.N. A new non-linear higher-order shear deformation theory for large-amplitude vibrations of laminated doubly curved shells. *Intern. J. Non-Linear Mech*. 2010. Vol. 45. P. 409–418. https://doi.org/10.1016/j.ijnonlinmec.2009.12.013.
19. Деревянко І., Аврамов К., Успенський Б., Саленко А. Експериментальний аналіз механічних характеристик деталей ракет-носіїв, виготовлених за допомогою FDM адитивних технологій. *Техн. механіка.* 2021. Вип. 1. С. 92–100. https://doi.org/10.15407/itm2021.01.092.
20. Duc N. D., Cong P.H., Tuan N. D., Tran P., Thanh N. V. Thermal and mechanical stability of functionally graded carbon nanotubes (FG CNT)-reinforced composite truncated conical shells surrounded by the elastic foundations. *Thin–Walled Structures*. 2017. Iss. 115. P. 300–310. https://doi.org/10.1016/j.tws.2017.02.016.